CONSTRAINED REORIENTATION OF SATELLITE FORMATIONS USING A QUASI-RIGID BODY FORMULATION

Christopher Blake[1] **and Arun K. Misra**[2]
Department of Mechanical Engineering
McGill University, Montreal, Quebec, Canada

Abstract

The quasi-rigid body formulation views a formation of satellites as a single entity by attaching a coordinate frame to the formation that captures its overall orientation. To begin, this paper reviews the formulation and presents the quasi-rigid body equations of motion. Then, a nonlinear controller for a formation is derived using Lyapunov stability theory. System performance criteria can be met by tuning the proportional and derivative feedback gains. Because the controller is based upon the quasi-rigid body equations of motion, it can be used to regulate orientation errors or track a time-varying trajectory for the attitude of the formation; this is shown through simulation results. Finally, the formulation is used to design two constrained reorientation trajectories for formations in deep space, one of which is a single Euler axis rotation, while the second is motivated by axisymmetric rigid body dynamics. It is shown that the second approach provides as much as 11% fuel savings over the Euler axis rotation.

1 INTRODUCTION

Much of the satellite formation flying literature has focused on leader-follower dynamics, however several studies have considered a formation as a single entity. Constellation templates [1] and the virtual structure approach [2] embed the satellites within a virtual body, while the virtual centre [3] captures the average translational motion of a formation. In a previous paper [4], the authors built upon the work of Cochran et al. [5], formalizing the quasi-rigid body (QRB) formulation, which is a framework for describing a formation so that it can be controlled as a rigid body. The formulation does this by attaching a coordinate frame to the formation that captures its overall orientation in space.

In this paper, it is shown how the formulation can be used to design a closed-loop nonlinear controller that acts on a formation as a whole. The stability and performance characteristics of this controller are discussed. Then the formulation is used to design constrained reorientation trajectories, which can be tracked by the controller. For deep space reorientations, rigid body theory is used to design a three-axis trajectory that is more fuel efficient than a single-axis rotation.

1.1 Quasi-Rigid Body Formulation

Summarizing the work of the previous paper [4], a satellite formation consists of N deputy satellites, numbered $i = 1 \ldots N$, moving relative to a chief satellite denoted by C. As shown in Figure 1, the inertial position of the i^{th} deputy is given by the vector $\mathbf{r}_i$, which can be expressed as the sum of the inertial position of the chief, $\mathbf{r}_c$, the known desired position of the i^{th} deputy with respect to the chief, $\mathbf{r}_{ni/c}$, and the deviation from that desired position, $\boldsymbol{\rho}_i$. If the trajectory of the chief is assumed to be known and the deputies are modelled as point masses, the generalized

[1]Master's Candidate, christopher.blake@mail.mcgill.ca
[2]Thomas Workman Professor and Chair, arun.misra@mcgill.ca

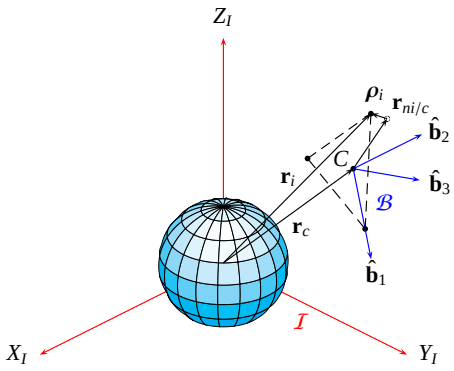

Figure 1: Deputy Satellites within the QRB Frame

coordinates and the generalized speeds for the satellite formation are, respectively,

$$\mathbf{q} = \begin{bmatrix} \boldsymbol{\rho}_1^T & \boldsymbol{\rho}_2^T & \dots & \boldsymbol{\rho}_N^T & \theta_1 & \theta_2 & \theta_3 \end{bmatrix}^T \tag{1}$$

$$\mathbf{p} = \begin{bmatrix} \mathring{\boldsymbol{\rho}}_1^T & \mathring{\boldsymbol{\rho}}_2^T & \dots & \mathring{\boldsymbol{\rho}}_N^T & \boldsymbol{\omega}_B^T \end{bmatrix}^T \tag{2}$$

where θ_1, θ_2, and θ_3 represent the attitude of the so-called QRB coordinate frame, and $\boldsymbol{\omega}_B$ is the angular velocity of that frame. The origin of this frame coincides with the centre of mass of the chief, and the axes of the frame are defined in terms of the relative positions of the deputies. From the previous paper, the x_B-axis is aligned with the line joining the chief to the first deputy and the y_B-axis lies in the plane formed by the chief and the first and second deputies. Because the system has only $3N$ degrees of freedom there are three excess coordinates, and so this definition necessarily imposes three constraints on the system. If the components of the i^{th} deviation vector in the QRB frame are labelled u_i, v_i, and w_i, the constraints are

$$v_1 = 0 \qquad w_1 = 0 \qquad w_2 = 0 \tag{3}$$

The QRB frame captures the bulk orientation of the satellite formation because it is defined in terms of the relative positions of the deputy satellites. By incorporating the attitude coordinates into the system description, and in turn the dynamics, the QRB formulation allows the design of controllers that can regulate the orientation of the satellite formation.

1.2 Equations of Motion

From Blake and Misra [4], the equations of motion (EOM) for a satellite formation derived using the QRB formulation are

$$\begin{aligned} \mathring{\mathring{\boldsymbol{\rho}}}_i - [\dot{\boldsymbol{\omega}}_B^\times]\mathbf{r}_{i/c} &= -2[\boldsymbol{\omega}_B^\times]\mathring{\mathbf{r}}_{i/c} - [\boldsymbol{\omega}_B^\times][\boldsymbol{\omega}_B^\times]\mathbf{r}_{i/c} - \mathring{\mathring{\mathbf{r}}}_{ni/c} \\ &\quad + \frac{1}{m_i}\mathbf{F}_i - \ddot{\mathbf{r}}_c\,, \qquad i = 1 \dots N \end{aligned} \tag{4a}$$

$$\begin{aligned} [I]\dot{\boldsymbol{\omega}}_B + \sum_{i=1}^{N} m_i[\mathbf{r}_{i/c}^\times]\mathring{\mathring{\boldsymbol{\rho}}}_i &= -2\sum_{i=1}^{N} m_i[\mathbf{r}_{i/c}^\times][\boldsymbol{\omega}_B^\times]\mathring{\mathbf{r}}_{i/c} - [\boldsymbol{\omega}_B^\times][I]\boldsymbol{\omega}_B \\ &\quad - \sum_{i=1}^{N} m_i[\mathbf{r}_{i/c}^\times]\mathring{\mathring{\mathbf{r}}}_{ni/c} - \sum_{i=1}^{N} m_i[\mathbf{r}_{i/c}^\times]\ddot{\mathbf{r}}_c + \boldsymbol{\Gamma} \end{aligned} \tag{4b}$$

$$\frac{d}{dt}\bar{q}_B = \frac{1}{2}[B(\bar{q}_B)]\boldsymbol{\omega}_B \tag{4c}$$

Superscript $^\times$ signifies a cross-product skew-symmetric matrix formed by the components of the vector the symbol modifies. $[I]$ is the inertia matrix that quantifies the mass distribution of the deputies about the chief. $\mathbf{F}_i$ is the sum of the forces experienced by the i^{th} deputy, including the gravitational force, perturbation forces, and control forces. $\mathbf{\Gamma}$ is the total torque about the chief satellite resulting from these forces. Eq. (4a) is the translational EOM for the i^{th} deputy, while Eq. (4b) is an angular momentum equation. If the deviation vectors, $\boldsymbol{\rho}_i$, are held to zero through some control effort, and if the chief is located at the centre of mass of the system, the second EOM collapses to Euler's rotational equation for a rigid body: $[I]\dot{\boldsymbol{\omega}}_B + [\boldsymbol{\omega}_B^\times][I]\boldsymbol{\omega}_B = \mathbf{\Gamma}$. Eq. (4c) relates the angular velocity to the time derivative of the attitude, given by the quaternion, $\bar{q}_B$.

Note that Eq. (4) contains $3N + 3$ differential equations. Again, because the system only has $3N$ degrees of freedom, the differential equations corresponding to deviation components $\ddot{v}_1$, $\ddot{w}_1$ and $\ddot{w}_2$ are dropped. Letting $\mathbf{\Upsilon}$ represent the nonlinear terms, in a condensed form, the EOMs are:

$$[M(\mathbf{q})]\dot{\mathbf{p}} = \mathbf{\Upsilon} + \begin{bmatrix}\mathbf{F}\\ \mathbf{\Gamma}\end{bmatrix} \tag{5}$$

where $[M(\mathbf{q})]$ is the symmetric mass matrix.

2 LYAPUNOV CONTROLLER

In this section, a nonlinear Lyapunov controller is designed. The technique of feedback linearization is used to cancel out nonlinear terms and obtain linear dynamic equations for the state error. Several simplifying assumptions are made for the controller design:

1. The mass of each satellite is much larger than the mass of onboard fuel. Therefore, the change in the system mass when fuel is expended can be neglected.
2. Onboard thrusters can produce continuous thrust in all three coordinate directions of the QRB frame.
3. The satellites can be treated as point masses.
4. The location of the chief satellite or reference point is known.
5. State measurements are perfect, i.e. there are no navigation errors.

2.1 Synthesis

Letting the subscript "D" stand for "desired," the desired orientation for the QRB frame is given by the quaternion, $\bar{q}_D$, while the desired angular velocity is $\boldsymbol{\omega}_D$. The desired position vector of the i^{th} deputy in the QRB frame is the nominal position vector, $\mathbf{r}_{ni/c}$. The errors in position and speed used for the Lyapunov controller are then

$$\Delta\mathbf{q} = \mathbf{q} - \mathbf{q}_D = [\boldsymbol{\rho}_1^T \quad \dots \quad \boldsymbol{\rho}_N^T \quad \boldsymbol{\epsilon}^T]^T \tag{6}$$

$$\Delta\mathbf{p} = \mathbf{p} - \mathbf{p}_D = [\mathring{\boldsymbol{\rho}}_1^T \quad \dots \quad \mathring{\boldsymbol{\rho}}_N^T \quad \boldsymbol{\omega}_{B/D}^T]^T \tag{7}$$

where $\boldsymbol{\omega}_{B/D}$ is the angular velocity of the QRB with respect to the desired frame, while $\boldsymbol{\epsilon}$ is the vector component of the quaternion, $\bar{q}_{B/D} = [q_0 \ \boldsymbol{\epsilon}^T]^T$, representing the error in orientation. When the components of this vector are all zero, the orientation error disappears. Thus, the goal of the controller is to drive the state error $\Delta\mathbf{x} = [\Delta\mathbf{q}^T \ \Delta\mathbf{p}^T]^T$ to zero making all the deviations, along with the orientation and angular velocity error, equal to zero. The speed error and the rate of change of the position error are related by:

$$\Delta\dot{\mathbf{q}} = [H]\Delta\mathbf{p} = \begin{bmatrix}[E_{(3N-3)\times(3N-3)}] & [0_{(3N-3)\times 1}]\\ [0_{1\times(3N-3)}] & \frac{1}{2}[B(\bar{q}_{B/D})]\end{bmatrix}\Delta\mathbf{p} \tag{8}$$

where $[B] = q_0[E] + [\boldsymbol{\epsilon}^\times]$ relates the angular velocity error to the quaternion error rate, with $[E]$ representing the identity matrix.

A candidate Lyapunov function for the system is selected as follows:

$$L = \frac{1}{2}\Delta\mathbf{p}^T\Delta\mathbf{p} + \frac{1}{2}\Delta\mathbf{q}^T[K]\Delta\mathbf{q} \tag{9}$$

where $[K]$ is a symmetric positive definite matrix. L is then a positive definite function of the system state, $\mathbf{x}$, about the desired state, $\mathbf{x}_D$. Setting the rate of change of this function equal to $-\Delta\mathbf{p}^T[P]\Delta\mathbf{p}$, where $[P]$ is also symmetric positive definite, makes $\dot{L}$ negative semi-definite so that L satisfies the criteria for a Lyapunov function. Then, by Lyapunov's Direct Method, the satellite formation described by the QRB EOMs is stable about the desired state trajectory.

The dynamic equation for the state error then becomes

$$\Delta\dot{\mathbf{p}} + [P]\Delta\mathbf{p} + [H]^T[K]\Delta\mathbf{q} = \mathbf{0} \tag{10}$$

By substituting Eqs. (5) and (7) into Eq. (10), the control vector can be solved:

$$\begin{bmatrix}\mathbf{F}_c\\ \boldsymbol{\Gamma}_c\end{bmatrix} = -[M(\mathbf{q})][H]^T[K]\Delta\mathbf{q} - [M(\mathbf{q})][P]\Delta\mathbf{p} - \boldsymbol{\Upsilon} + [M(\mathbf{q})]\dot{\mathbf{p}}_D \tag{11}$$

Eq. (11) is the Lyapunov controller. The role of each term in this control expression is apparent. The first term is the position error feedback while the second term is the velocity error feedback. The selection of matrices $[K]$ and $[P]$ determines the dynamics of the state error. Subtracting $\boldsymbol{\Upsilon}$ cancels out the nonlinear terms of the dynamic equation, and so it provides feedback linearization. The last term is the control effort needed to maintain the desired state trajectory. Using the Higher Derivative Theorem [6], it can be shown that this controller is asymptotically stable. Thus, provided $\boldsymbol{\Upsilon}$ accurately models the nonlinear dynamics (gravity, perturbations), any deviations or orientation errors will be driven to zero by the controller.

The Lyapunov controller prescribes a control thrust for each deputy, $\mathbf{F}_{ci}$, having components along the three coordinate directions, with the exception of deputies 1 and 2. Because components v_1, w_1, and w_2 are constrained, no thrust is prescribed in those directions. However, the controller does prescribe a control torque, $\boldsymbol{\Gamma}_c$, to be applied to the QRB. This torque must be obtained by distributing thrusts among the deputies that define the QRB frame, that is, by thrusting in the remaining coordinate directions for deputies 1 and 2. Hence, $3N$ thrust components are fully specified by this controller.

Assuming that $[K]$ and $[P]$ are block diagonal gain matrices, according to Eq. (11), the control forces applied to deputies numbered $i > 2$ are determined by their own state errors, the state of the chief, but also by the states of deputies 1 and 2, as these determine the orientation error of the QRB frame. Since the control torque is also determined by the orientation error of the QRB frame, this means that the control forces applied to deputies 1 and 2 are determined by the states of both deputies. There is interdependency between deputies 1 and 2, making this controller *cyclic* [7]. If more deputies are involved in the definition of the QRB frame, more dependencies between deputies result, and controlling the QRB frame affects more of the satellites.

2.2 Gain Selection

If the feedback gain matrices, $[K]$ and $[P]$, are diagonal, and if $[B]^T \approx [E]$ for small orientation error, the dynamic equation for the error, Eq. (10), can be decoupled into second-order linear constant-coefficient differential equations. For the deviation errors, $\boldsymbol{\rho}_i$, the natural frequency and damping ratio are $\varpi_n = \sqrt{K_i}$ and $\zeta = P_i/(2\sqrt{K_i})$ while for the orientation error, $\boldsymbol{\epsilon}$, they are $\varpi_n = \sqrt{K_\omega}/2$ and $\zeta = P_\omega/\sqrt{K_\omega}$. Provided the damping ratio, ζ, is less than 1, the settling time for the error is $T_s \approx 4/(\varpi_n\zeta) = 8/P$. Hence, the values along the diagonal for matrices $[K]$ and $[P]$ can be chosen so that the system meets imposed performance specifications.

3 REORIENTATION

A *constrained* reorientation is a slew manoeuvre during which the deputy satellites maintain constant relative positions within the QRB frame. There could be several reasons to do this: scientific data collection is to occur during reorientation, collision avoidance is an important mission requirement, or as mentioned by Beard et al. [8], for interferometry missions, formation acquisition can be timely and fuel intensive, so sensor lock between satellites should be maintained. In this section, three constrained reorientation trajectories are developed. The Lyapunov controller can then be used to track these trajectories.

3.1 Single-Axis Rotation

In a deep space environment, the purpose of reorienting a formation would be to image different celestial targets. Differential gravity is negligible in deep space, and a formation can be at "rest". The only forces acting on the satellites are control forces, so in Eq. (4), $\mathbf{F}_i = \mathbf{F}_{ci}$ and $\mathbf{\Gamma} = \mathbf{\Gamma}_c$.

Consider an initial inertial attitude for the QRB frame, $\bar{q}_{D0}$ and a final attitude, $\bar{q}_{Df}$. With a step change in the desired attitude, the Lyapunov controller will correct the error, reorienting the QRB frame while maintaining the shape of the formation. The rate at which the slew occurs will depend upon the gains of the controller. To more actively specify the rate of slew, a continuously time-varying orientation for the QRB frame to follow can be specified.

Consider, then, the change in inertial orientation, $\bar{q}_{f/0}$, from which the Euler axis, $\hat{\mathbf{e}}$, and Euler angle, Φ_f, can be extracted. A constant rotation rate for the formation about that axis over some time period $[t_0,\ t_f]$ can be prescribed so that the slew angle increases linearly with time:

$$\Phi(t) = \begin{cases} 0 & t < t_0 \\ \Phi_f \frac{t-t_0}{t_f-t_0} & t_0 < t < t_f \\ \Phi_f & t > t_f \end{cases} \tag{12}$$

The corresponding desired angular velocity trajectory is $\boldsymbol{\omega}_D = \dot{\Phi}(t)\hat{\mathbf{e}}$. Each deputy satellite will need to be provided with a centripetal acceleration, directed along the perpendicular line connecting it with the Euler axis. Assuming the Euler axis passes through the origin of the QRB frame, the total fuel consumption in terms of Δv can be shown to be

$$\Delta v_T = \sum_{i=1}^{N} \left\{ \frac{\Phi_f^2}{t_f - t_0} \|\mathbf{r}_{ni/c} - \mathbf{r}_{ni/c} \cdot \hat{\mathbf{e}}\| + 2\frac{\Phi_f}{t_f - t_0} \|\mathbf{r}_{ni/c} \times \hat{\mathbf{e}}\| \right\} \tag{13}$$

It is noted that this single-axis manoeuvre is not motivated by any dynamics.

3.2 Three-Axis Rotation

To reduce fuel consumption, a constrained reorientation should take advantage of the inherent dynamics of the system. If deputy satellites of equal mass are symmetrically distributed about the chief, then the theory of axisymmetric bodies can be employed. It was shown by Dixon et al. [9] that under certain assumptions, the fuel-optimal trajectory for the rest-to-rest reorientation of an axisymmetric rigid body consists of a series of patched coasting arcs. Limiting the control effort to two unbounded impulses – one to initiate the manoeuvre, and one to terminate it – the trajectory follows the natural torque-free precession-nutation-spin motion of the body. The same idea can be applied to a satellite formation.

It is assumed that the deputy satellites are fixed within the QRB frame and that the formation is in a deep space environment. Let ψ be the precession angle about an inertially fixed axis parallel to some unit vector, $\hat{\mathbf{h}}$, passing through the centre of mass of the axisymmetric QRB. Let ϑ

be the nutation angle and ϕ be the spin angle about the body-fixed z_B-axis. The motion of the axisymmetric QRB in terms of these 3-1-3 Euler angles is given by [9]

$$\begin{aligned} \vartheta &= \vartheta(t_0) \\ \psi(t) &= \frac{H}{I_t}(t - t_0) \\ \phi(t) &= \psi(t)\left(\frac{I_t}{I_a} - 1\right)\cos\vartheta + \phi(t_0) \\ &= c(t - t_0) + \phi(t_0) \end{aligned} \tag{14}$$

$\mathbf{H} = H\hat{\mathbf{h}}$ is the angular momentum of the QRB, which is constant since the motion is torque-free. I_t and I_a are the transverse and axial moments of inertia respectively, extracted from the inertia matrix, $[I]$. The angular velocity of the QRB frame expressed in that frame is

$$\begin{bmatrix} \omega_1(t) \\ \omega_2(t) \\ \omega_3(t) \end{bmatrix} = \begin{bmatrix} \cos c(t-t_0) & \sin c(t-t_0) & 0 \\ -\sin c(t-t_0) & \cos c(t-t_0) & 0 \\ 0 & 0 & 1 \end{bmatrix} \underbrace{\begin{bmatrix} \frac{H}{I_t}\sin\vartheta\sin\phi(t_0) \\ \frac{H}{I_t}\sin\vartheta\cos\phi(t_0) \\ \frac{H}{I_a}\cos\vartheta \end{bmatrix}}_{\omega_B(t_0)} \tag{15}$$

where $c = (1 - I_a/I_t)\omega_3(t_0)$. For a given inertial reorientation, $\bar{q}_{f/0}$, the nutation angle, ϑ, unit vector, $\hat{\mathbf{h}}$, and initial conditions at $t = t_0$ can be obtained.

The theory of axisymmetric rigid bodies establishes the torque-free coasting arc for the re-orientation manoeuvre, but for a QRB, fuel is still expended during the manoeuvre to maintain the rigid configuration. Setting the deviations identically to zero in Eq. (4a) with no gravity or perturbation terms, the open-loop fuel consumption, in terms of Δv, can be calculated by:

$$\sum_{i=1}^{N}\int_{t_0}^{t_f} \|\mathbf{a}_i\| dt = \sum_{i=1}^{N}\int_{t_0}^{t_f} \|\dot{\boldsymbol{\omega}}_B \times \mathbf{r}_{ni/c} + \boldsymbol{\omega}_B \times (\boldsymbol{\omega}_B \times \mathbf{r}_{ni/c})\| \tag{16}$$

An impulsive "torque" provides the QRB with an angular momentum to initiate the manoeuvre, and then another removes it to terminate the manoeuvre. This translates to a change in inertial velocity for each deputy at the beginning and end of the manoeuvre. The total fuel consumption is then

$$\Delta v_T = \sum_{i=1}^{N}\left\{\int_{t_0}^{t_f} \|\mathbf{a}_i\| dt + 2\|\mathbf{r}_{ni/c} \times \boldsymbol{\omega}_B(t_0)\|\right\} \tag{17}$$

4 SIMULATIONS

A satellite formation consisting of $N = 3$ deputies was simulated using Matlab. The deputies were assigned equal masses of 100 kg each, and distributed symmetrically within the XY plane of the QRB frame a distance $R = 1$ km from the chief to form an equilateral triangle. Newton's Second Law was used to represent the dynamics of each satellite: $m_i\ddot{\mathbf{r}}_i = \mathbf{F}_i$. However, the Lyapunov controller based on the QRB EOMs was used to track the desired trajectory for the formation.

Three examples of a constrained reconfiguration in a deep space environment were compared for an orientation change given by the direction cosine matrix $[R_x(\pi/2)][R_y(\pi/2)]$. Subscripts x and y signify body-fixed rotations about those axes. The formation was simulated with the feedback gain matrices set to $[K] = 64 \times 10^{-8}[E]$ and $[P] = 7 \times 10^{-4}[E]$. The time interval for the manoeuvres was 20000 seconds.

Table 1: Comparison of Fuel Consumed by Euler Axis and Three-Axis Deep Space Manoeuvres

	Δv (m/s)						
	Step	Analytical		$\kappa = 0.1$		$\kappa = 0.5$	
		Euler	3-Axis	Euler	3-Axis	Euler	3-Axis
Sat 1	0.5188	0.3501	0.3217	0.3695	0.3418	0.4921	0.4646
Sat 2	0.6211	0.4191	0.4105	0.4423	0.4375	0.5891	0.6007
Sat 3	0.3907	0.2636	0.2139	0.2782	0.2208	0.3705	0.2727
Total	1.5306	1.0328	0.9462	1.0901	1.0002	1.4517	1.3380

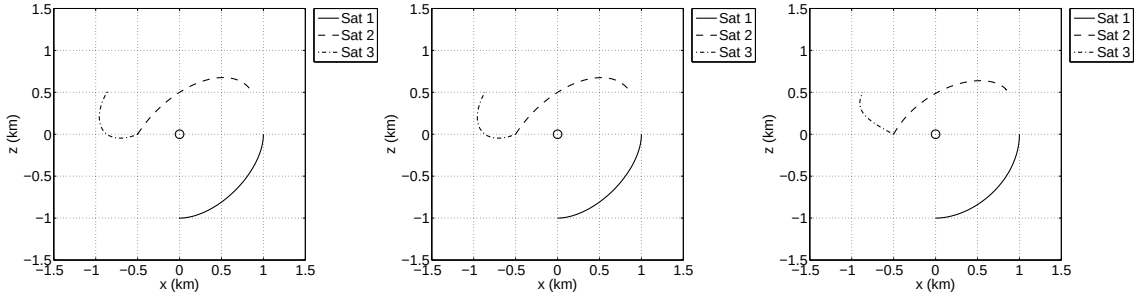

(a) Step Reorientation (b) Euler Axis Rotation (c) Three-Axis Rotation

Figure 2: Comparison of Satellite Trajectories for Deep Space Manoeuvres

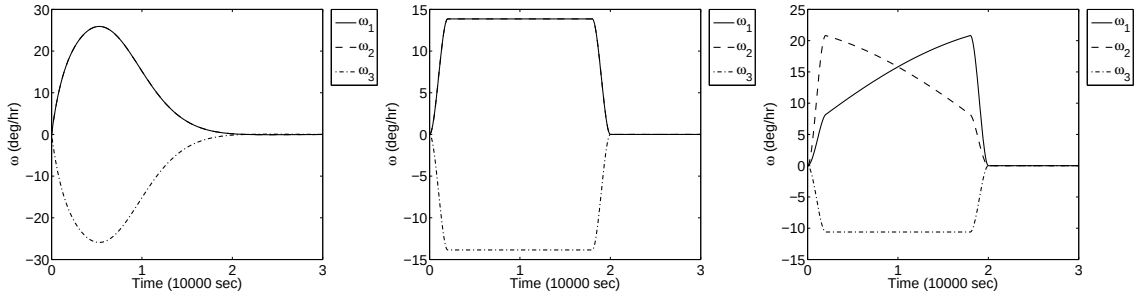

(a) Step Reorientation (b) Euler Axis Rotation (c) Three-Axis Rotation

Figure 3: Comparison of Angular Velocity for Deep Space Manoeuvres, $\kappa = 0.1$

Table 1 compares the fuel consumed by the satellites for a step change in the desired orientation, for a single rotation about the Euler axis, and for the combined precession-spin motion of the three-axis manoeuvre. The theoretical fuel requirements, as calculated by Eqs. (13) and (17) are compared with simulation results. Note that Eqs. (12) and (14) prescribe linear changes in orientation angles, ramping from an initial value to a final value. This corresponds to a sudden change in the angular rates of the QRB frame, necessitating a sudden change in the momentum of each deputy. To avoid near impulsive control forces, the ramp is smoothed at the beginning and end of the manoeuvre. κ represents the fraction of the manoeuvre time over which there is smoothing.

From the results, it can be seen that the step manoeuvre consumed the most fuel. A smaller smoothing factor, κ, reduced the fuel consumption of the Euler axis and three-axis manoeuvres. The three-axis manoeuvre consumed less total fuel than the Euler axis manoeuvre. Fuel consumption was not balanced across the deputies.

Figure 2 compares the three-dimensional (3D) trajectories followed by the three deputies, while Figure 3 compares the angular velocity of the QRB frame for the three manoeuvres, with $\kappa = 0.1$. With the step reorientation, the QRB frame actually rotates about the Euler axis, generating the same 3D trajectory as the Euler axis rotation. However, as shown in Figures 3a and 3b, the rate of rotation differs, which explains the difference in fuel consumption. For the three-axis manoeuvre, the 3D trajectory is different (Figure 2c). Comparing Figures 3b and 3c, for the Euler axis manoeuvre, the angular velocity was constant in the middle of the manoeuvre, whereas it varied for the three-axis manoeuvre. This change provided the fuel savings.

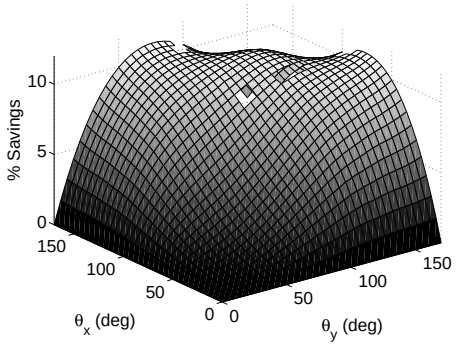

Figure 4: Percentage Fuel Savings of Three-Axis Deep Space Manoeuvre

To fully quantify the advantage of the three-axis manoeuvre over the Euler axis manoeuvre, Figure 4 plots the percent savings in fuel for a general final orientation $[R_x(\theta_x)][R_y(\theta_y)]$, as calculated by Eqs. (13) and (17). For small changes in orientation, the advantage is small. In fact, the manoeuvres are identical when the rotation is only about the x_B-axis or only the y_B-axis. But, for $\theta_x = 170^\circ$ and $\theta_y = 75^\circ$, there is a maximum total fuel savings of 11%. The savings is independent of the manoeuvre time.

5 CONCLUSION

This paper presented the design of a nonlinear controller based upon the equations of motion from the QRB formulation. The advantage of this controller is that it acts upon a satellite formation as a whole, regulating the attitude of the formation. Simulations showed that the controller could correct orientation errors as well as track time-varying trajectories for the attitude. This paper presented two such trajectories and showed that the three-axis reorientation trajectory obtained from axisymmetric rigid body dynamics offers fuel savings for large angle manoeuvres.

REFERENCES

[1] Beard, R. W. and Hadaegh, F. Y., "Constellation Templates: An Approach To Autonomous Formation Flying," *World Automation Congress*, ISIAC, Anchorage, AK, USA, May 1998.

[2] Ren, W. and Beard, R. W., "Decentralized Scheme for Spacecraft Formation Flying via the Virtual Structure Approach," *Journal of Guidance, Control, and Dynamics*, Vol. 27, No. 1, 2004, pp. 73–82.

[3] Tillerson, M., Breger, L., and How, J. P., "Distributed Coordination and Control of Formation Flying Spacecraft," *American Control Conference*, Vol. 2, IEEE, June 2003, pp. 1740–1745.

[4] Blake, C. and Misra, A. K., "Dynamics and Control of Satellite Formations using a Quasi-Rigid Body Formulation," *AAS/AIAA Space Flight Mechanics Meeting*, Vol. 130 of *Advances in the Astronautical Sciences*, Galveston, TX, USA, Jan. 2008, pp. 691–710.

[5] Cochran, Jr., J. E., Aoki, H., and Choe, N., "Modeling Closely-Coupled Satellite Systems as Quasi-Rigid Bodies," *AAS/AIAA Space Flight Mechanics Meeting*, Vol. 119 of *Advances in the Astronautical Sciences*, Maui, HI, USA, Feb. 2004, pp. 1349–1368.

[6] Schaub, H. and Junkins, J. L., *Analytical Mechanics of Space Systems*, AIAA Education Series, AIAA, Reston, VA, USA, 2003.

[7] Scharf, D. P., Hadaegh, F. Y., and Ploen, S. R., "A Survey of Spacecraft Formation Flying Guidance and Control (Part II): Control," *American Control Conference*, Vol. 4, IEEE, Boston, June 2004, pp. 2976–2985.

[8] Beard, R. W., McLain, T. W., and Hadaegh, F. Y., "Fuel Equalized Retargeting for Separated Spacecraft Interferometry," *American Control Conference*, Vol. 3, IEEE, Philadelphia, PA, USA, June 1998, pp. 1580–1584.

[9] Dixon, M. V., Edelbaum, T. N., Potter, J. E., and Vandervelde, W. E., "Fuel optimal Reorientation of Axisymmetric Spacecraft," *Journal of Spacecraft and Rockets*, Vol. 7, No. 11, 1970, pp. 1345–51.